Size and Polydispersity Determinations of AOT/Bile Salt Reversed Micelles Obtained by Small-Angle Neutron Scattering

K. S. Freeman,[†] N. C. Beck Tan,[‡] S. F. Trevino,[‡,§] S. Kline,[§] L. B. McGown,[†] and D. J. Kiserow*[,||]

Department of Chemistry, Box 90346, Duke University, Durham, North Carolina 27708-0346, U. S. Army Research Laboratory, Materials Division, Building 4600, Aberdeen Proving Ground, Maryland 21005, Center for Neutron Research, National Institute of Standards and Technology, REACT E151, Gaithersburg, Maryland 20899, and U. S. Army Research Office, Chemical Sciences Division, P.O. Box 12211, Research Triangle Park, North Carolina 27709-2211

Received February 5, 2001. In Final Form: March 30, 2001

Previous work has shown that trihydroxy bile salt cosurfactants significantly modify the interfacial properties and aggregate size of Aerosol-OT (AOT) reversed micelles and can also increase the activity of enzymes such as chymotrypsin and lipase that are solubilized in the AOT reversed micelles. In the present work, small-angle neutron scattering (SANS) was used to study the effects of one such bile salt, sodium taurocholate (NaTC), on the size and polydispersity of AOT reversed micelles. At low concentrations, NaTC decreases the overall size of the reversed micelles, the size of the interior water pools, and the apparent thickness of the detergent layer, while causing an increase in polydispersity. At higher NaTC concentrations, the overall aggregate size, the size of the water pools, the thickness of the detergent layer, and the polydispersity all are increased. It is proposed that, at low concentrations, NaTC monomers are randomly dispersed among the AOT molecules in a perpendicular orientation, thereby disrupting the organization of the detergent layer and increasing penetration of heptane and water into the detergent layer. When NaTC is increased, it may form hydrogen-bonded dimers that are aligned parallel to the AOT molecules. In this orientation, there is less disruption of the detergent layer and penetration of heptane and water molecules is reduced. Finally, it was found that reversed micelles containing chymotrypsin are smaller than unoccupied aggregates, suggesting structural reorganization in order to accommodate the protein. From these results, the effects of NaTC on chymotrypsin activity in AOT reversed micelles can be attributed to structural and chemical modification of the detergent layer rather than to changes in the overall dimensions of the reversed micelles.

Introduction

Aerosol-OT (AOT) reversed micelles can be used to solubilize large biological molecules over a broad concentration range of water in organic solvents. This has led to numerous investigations of the mechanisms by which encapsulation of enzymes in reversed micelles affects their catalytic behavior.[1−9] Our efforts have focused on further enhancement of enzyme catalysis in AOT reversed micelles through the addition of trihydroxy bile salt cosurfactants such as sodium taurocholate (NaTC). Bile salts alone do not form stable aggregates in apolar solvents. We have previously shown, however, that addition of NaTC significantly modifies the physical and chemical properties of AOT reversed micelles.[10,11] Furthermore, we found that NaTC and the zwitterionic bile salt CHAPS can increase the enzymatic activity of chymotrypsin and lipase in AOT reversed micelles.[12,13] To achieve a better understanding of the effects that bile salts have on enzymatic catalysis in AOT reversed micelles, it is important to understand their effects on the physicochemical nature of the reversed micellar aggregates.

This paper describes the results of small-angle neutron scattering (SANS) experiments that were performed to gain insight into the effects of NaTC on the overall size and polydispersity of AOT reversed micelles, the size of the water pools, and the thickness of the AOT detergent layer. The effects of chymotrypsin encapsulation were studied as well, in the absence and presence of NaTC. SANS has been extensively applied to studies of AOT reversed micelles[14−19] and bile salt aggregation and transport in aqueous solution[20−23] but never before to the AOT/bile salt reversed micellar system.

* To whom correspondence should be addressed.
[†] Duke University. E-mail: lbmcgown@chem.duke.edu.
[‡] U. S. Army Research Laboratory.
[§] National Institute of Standards and Technology.
[||] U. S. Army Research Office.

(1) Luisi, P. L., Straub, B., Eds. *Reverse Micelles*; Plenum: New York, 1984.
(2) Menger, F. M.; Yamada, K. *J. Am. Chem. Soc.* **1979**, *101*, 6731.
(3) Barbaric, S.; Luisi, P. L. *J. Am. Chem. Soc.* **1981**, *103*, 4239.
(4) Wolf, R.; Luisi, P. L. *Biochem. Biophys. Res. Commun.* **1979**, *89*, 209.
(5) Pileni, M. P., Ed. *Structure and Reactivity in Reverse Micelles*; Elsevier: New York, 1989.
(6) Luisi, P. L. *Angew. Chem.* **1985**, *24*, 439.
(7) Mozhaev, V. V.; Khmelnitsky, Y. L.; Sergeeva, M. V.; Belova, A. B.; Klyachko, N. L.; Levashov, A. V.; Martinek, K. *Eur. J. Biochem.* **1989**, *184*, 597.
(8) Luisi, P. L.; Steinmann-Hofmann, B. *Methods Enzymol.* **1987**, *136*, 188.
(9) Fletcher, P. D. I.; Freedman, R. B.; Mead, J.; Oldfield, C.; Robinson, B. H. *Colloids Surf.* **1984**, *10*, 193.
(10) Lee, S. S.; Rideau, A. M.; McGown, L. B. *J. Phys. Chem.* **1996**, *100*, 5880.
(11) Lee, S. S.; Kiserow, D. J.; McGown, L. B. *J. Colloid Interface Sci.* **1997**, *193*, 32.
(12) Freeman, K. S.; Lee, S. S.; Kiserow, D. J.; McGown, L. B. *J. Colloid Interface Sci.* **1998**, *207*, 344.
(13) Freeman, K. S.; Tang, T. T.; Shah, R. D. E.; Kiserow, D. J.; McGown, L. B. *J. Phys. Chem. B* **2000**, *104*, 9312.
(14) Feigin, L. A.; Svergun, D. I. *Structure Analysis by Small-Angle X-ray and Neutron Scattering*; Plenum: New York, 1987.

10.1021/la0101797 CCC: $20.00
Published on Web 05/31/2001

Experimental Section

Materials.[24] AOT (bis(2-ethylhexyl)sulfosuccinate, sodium salt, BioChemika MicroSelect, Fluka), NaTC (sodium salt, ULTROL grade, >98%, Calbiochem), α-chymotrypsin (Type II from bovine pancreas, Sigma), *d*-heptane, and D_2O (>99.9%, Cambridge Isotope Laboratories) were all used as received.

The reversed micelle solutions were prepared as follows: H_2O (HPLC grade) or D_2O was added to a stock solution of 40 mM AOT in deuterated heptane and stirred on a magnetic stir plate until the solutions were clear. These solutions were then added to solid NaTC and stirred until the cosurfactant was completely solubilized. Approximately 2 h of stirring are required for the higher NaTC concentrations. Alternatively, stock solutions of enzyme in water were added to the AOT/solvent solutions prior to the solubilization of the cosurfactant. In all cases the ω value (ω = [H_2O or D_2O]/[AOT]) was 10.

Instrumentation. Small-angle neutron scattering measurements were performed at the National Institute of Standards and Technology Center for Neutron Research in Gaithersburg, MD, using the 30 m SANS spectrometer located at NG-7. Samples were contained in 1 mm path length quartz cells and maintained at 25.0 ± 0.2 °C. The scattering intensity was measured as a function of Q, the magnitude of the scattering vector. Q is related to the scattering angle, Θ, by[14]

$$Q = 4\pi \sin(\Theta/2)/\lambda \quad (1)$$

λ is the wavelength of the incident neutron beam (λ = 6 Å for these experiments).

The detector was a 64 × 64 cm^2 He-3 position-sensitive proportional counter with 1 cm^2 resolution. Q values were measured for 0.05−0.5979 $Å^{-1}$, with the detectors positioned at 1, 4, and 13 m from the sample. Data were corrected for the scattering from an empty quartz sample cell, the detector background and sensitivity, the transmission of each sample, and the scattering resulting from the deuterated organic solvents. Absolute scattering intensities were obtained by reduction of the raw data through calibration with secondary standards of known cross section. Water was used as the calibration standard for measurements with the detector positioned at 1 m, and a Sil B2 silica standard was used at 4 and 13 m.

Theory. The small-angle scattering intensity, $I(Q)$, from an assembly of particles dispersed in a solvent may be represented by the expression

$$I(Q) = NK_iP(Q)\,S(Q) \quad (2)$$

where N is the number of scattering particles, K_i is a contrast factor for radiation of type i, $P(Q)$ is the intraparticle scattering function for a single particle, and $S(Q)$ is a scattering function for interparticle correlations.[14,15] For non-interacting particles in dilute solution, the intraparticle contribution dominates the scattering. Under these conditions, the function $S(Q)$ approaches unity, simplifying eq 2 to

$$I(Q) = NK_iP(Q) \quad (3)$$

Thus, the form of the scattered intensity, $I(Q)$, from a dilute solution of non-interacting particles as a function of the scattering vector, Q, is defined by the function $P(Q)$, while the magnitude of the scattered intensity is controlled by K_i.

The contrast factor, K_i, in any system is directly related to the differences in the neutron scattering lengths of the components (i.e., the particle and the solvent). Since the neutron scattering lengths of hydrogen and deuterium are dramatically different, -0.3739×10^{-12} and 0.6671×10^{-12} cm, respectively,[16] deuterium labeling is an excellent means for generating neutron contrast. Two types of deuterium contrasting mechanisms were used in this study. In the first, the micelles were prepared with protonated water cores in deuterated bulk organic solvents. This defines the particle as the entire micelle, surfactant layer plus core, and allows study of overall aggregate size. In the second contrasting mechanism, the micelles were prepared in deuterated bulk organic solvents with deuterated water cores. This defines the remaining protonated component of the system, the detergent layer, as the "particle". Comparison of the results of the two contrasting mechanisms allows the exploration of changes in the micellar inner core.

Returning to eq 2, one sees that while K_i defines which species in the system constitutes a particle, all of the information regarding the structure of the particle is contained in $P(Q)$. The goal of the present work was to study the dimensions of the reversed micelles prepared with different NaTC and enzyme concentrations, which is information contained within $P(Q)$. The micellar dimensions may be extracted in two ways. The particle radius can be obtained directly from Guinier analysis of the data, or particle dimensions may be extracted from a nonlinear fit of the scattering data to an appropriate structure factor model. In either case, the overall shape of the reversed micelles must be assumed prior to performing the fit. Models can be used assuming spherical, rodlike, or cylindrical reversed micelles. In this work, among the different geometries the data were best fit to a spherical model.

The first method is based on the Guinier approximation. For scattering from a dilute solution of non-interacting particles in the limit of low Q, the scattered intensity, $I(Q)$, is simply related to $(R_gQ)^2$, where R_g is the radius of gyration of the particle. For scattering from a particle with spherical symmetry, the Guinier approximation is appropriate for analysis of scattering data,[14] and the function $P(Q)$ takes the form

$$P_{\text{Guinier}}(Q) = \exp\left[-\frac{Q^2R_g^2}{3}\right] \quad (4)$$

Combining eqs 3 and 4 allows extraction of R_g from the slope of the linear portion of a plot of $\ln(I(Q))$ versus Q^2. When scattering contrast was acquired by using protonated water, the radius of the entire reversed micelle (water pool + surfactant layer) could be calculated from R_g according to the equation for a sphere with radius R_1:[14]

$$R_g^2 = 3R_1^2/5 \quad (5)$$

Alternatively, when deuterated water was used, R_g is related to a spherical shell with outer radius R_1 and inner radius R_2:[14]

$$R_g^2 = \frac{3}{5}\frac{R_1^5 - R_2^5}{R_1^3 - R_2^3} \quad (6)$$

The Guinier approximation is strictly valid only in the range in which $QR_g \ll 1$. Though practical considerations generally prohibit the collection of scattering data in the extreme limit of low Q, the Guinier approximation generally gives estimates which are accurate to within 5−10% if the analysis is conducted using data collected within the range where $QR_g \sim 1$. Reliance on low Q data to extract the particle dimensions makes the Guinier estimates more sensitive to larger species in the system.

(15) Hammouda, B. *A Tutorial on Small-Angle Neutron Scattering from Polymers*; National Institute of Standards and Technology, Materials Science and Engineering Laboratory: Gaithersburg, MD, 1997.
(16) Sears, V. F. *Neutron News* **1992**, *3*, 26.
(17) Kaler, E. W.; Billman, J. F.; Fulton, J. L.; Smith, R. D. *J. Phys. Chem.* **1991**, *95*, 458.
(18) Sheu, E.; Goklen, K. E.; Hatton, T. A.; Chen, S. H. *Biotechnol. Prog.* **1986**, *2*, 175.
(19) Mueller, A.; Lang, P.; Findenegg, G. H.; Keiderling, U. *J. Phys. Chem. B* **1998**, *102*, 8958.
(20) Hjelm, R. P.; Thiyagarajan, P.; Alkan, H. *J. Appl. Crystallogr.* **1988**, *21*, 858.
(21) Hjelm, R. P.; Alkan, M. H.; Thiyagarajan, P. *Mol. Cryst. Liq. Cryst.* **1990**, *180A*, 155.
(22) Hjelm, R. P.; Thiyagarajan, P.; Alkan-Onyuksel, H. *J. Phys. Chem.* **1992,** *96*, 8653.
(23) Hjelm, R. P.; Schteingart, C.; Hofmann, A. F.; Sivia, D. S. *J. Phys. Chem.* **1995**, *99*, 16395.
(24) Certain commercial materials and equipment are identified in this paper in order to specify adequately the experimental procedure. In no case does such identification imply recommendation by the National Institute of Standards and Technology nor does it imply that the material or equipment identified is necessarily the best available for this purpose.

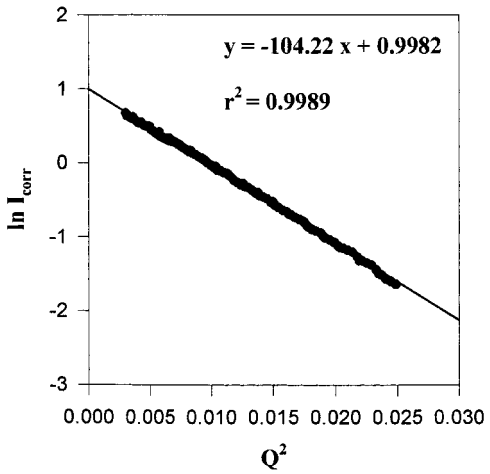

Figure 1. Plot of the linear region of the ln(I) versus Q^2 plot for 5 mM NaTC, deuterated core micelles in heptane. The line through the data represents the linear least-squares fit to the data that is used to extract the radius of gyration R_g.

The second method for determining the geometry of the reversed micelles involves a nonlinear fit of the data with the parameters of a specific model. This model describes the structure factor, $P(Q)$, due to isolated, non-interacting micelles. The model used in this work consists of a spherical core of a known neutron contrast whose radius conforms to a polydispersity described by a Schultz distribution.[25] This core is surrounded by a shell of constant thickness, T, again having known but different neutron contrast. The micelle exists in a liquid of yet a third neutron contrast. The parameters of the model are thus R_1, the most probable core radius, $R_2 = R_1 + T$, and the polydispersity of the Schultz distribution as a fraction of R_1. Thus, this method generates values for the average core radius, the core polydispersity, and the shell thickness (thickness of the surfactant layer). Polydispersity values range from 0 to 1, with a monodisperse system having a value of 0.

Because polydispersity is factored into the determination, nonlinear methods often yield more reliable assessments of particle size than Guinier plots. In addition, all of the data are used in the nonlinear fitting method, as compared to only the data collected at very small Q values for the Guinier analysis.

Nonlinear curve fitting was performed using commercial software with a polydisperse spheres macro that factors in the scale, the instrumental background, and the scattering length densities of all materials in solution. When performing the fit, the parameters are set to calculated values and the model converges on the scattering intensity data based on a Schulz distribution of particle size by varying the core radius, the core polydispersity, and the shell thickness. For samples that contain a protonated water core, the shell thickness must be set to zero because there is insufficient contrast between protonated surfactant molecules and protonated water pools.

Results

Guinier Analysis. Figure 1 shows a typical example of a Guinier fit to a plot of ln($I(Q)$) versus Q^2, and Table 1 gives a summary of the results for particle radii as a function of NaTC and chymotrypsin. The addition of 5 mM NaTC decreases both the overall size of the reversed micelles and, to a smaller degree, the size of the interior water pools. At 10 mM NaTC, the overall radius is the same as the radius of the reversed micelles without NaTC, although the water pool is considerably larger than that in 0 or 5 mM NaTC. At 20 mM NaTC, the overall size of the aggregates is larger than that in the other solutions although the water pool is similar to that in 10 mM NaTC.

(25) Degiorgio, V., Lorti, M., Eds.; *Physics of Amphiphiles, Micelles, Vesicles and Macroemulsions*; Elsevier Science Ltd.: New York, 1985.

Table 1. Results of Size Determinations in Heptane Obtained from Guinier Plots[a]

sample	R_1	R_2
0 mM NaTC	28.4 ± 0.1	17.4 ± 0.3
5 mM NaTC	22.8 ± 0.1	16.1 ± 0.2
10 mM NaTC	28.5 ± 0.1	21.5 ± 0.5
20 mM NaTC	31.7 ± 0.2	22.3 ± 0.6
0 mM NaTC/chymotrypsin	22.6 ± 0.1	
10 mM NaTC/chymotrypsin	25.5 ± 0.1	

[a] R_1 and R_2 are radii (in Å) of the overall reversed micelles and interior water pools, respectively. R_2 values for samples with chymotrypsin could not be determined because the core cannot be deuterated.

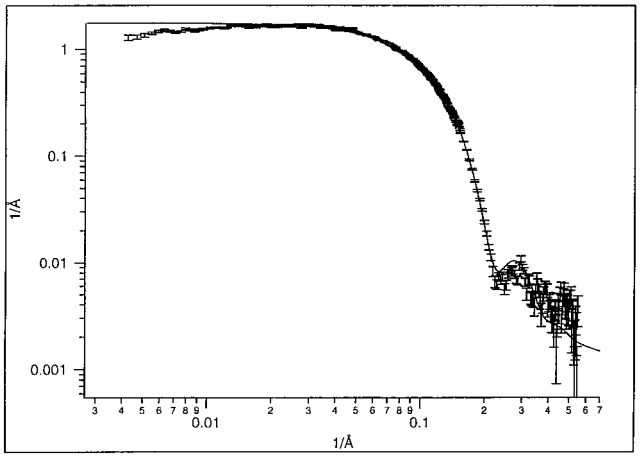

Figure 2. Plot of log I versus log Q (represented by convention as 1/Å versus 1/Å) for AOT reversed micelles in heptane with 5 μM chymotrypsin and 0 mM NaTC. The measured absolute intensity is represented by the data points with standard deviation error bars. The polydisperse spheres model fit to the data is represented by the solid line.

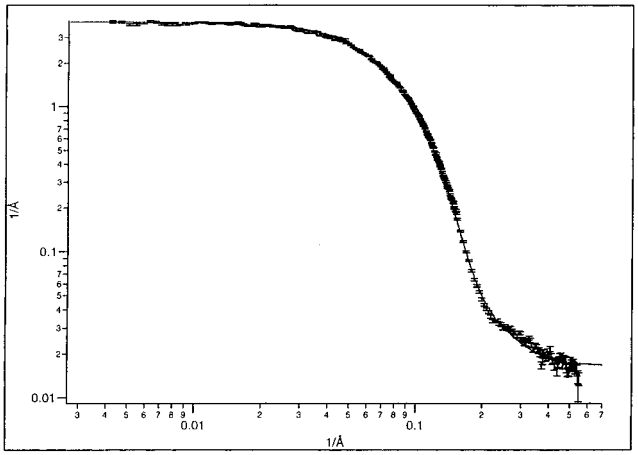

Figure 3. Plot of log I versus log Q (represented by convention as 1/Å versus 1/Å) for AOT reversed micelles in heptane with 5 μM chymotrypsin and 10 mM NaTC. The measured absolute intensity is represented by the data points with standard deviation error bars. The polydisperse spheres model fit to the data is represented by the solid line.

The results also show that the thickness of the surfactant layer decreases by almost 50% upon addition of 5−10 mM NaTC but increases upon further addition of NaTC until, at 20 mM NaTC, it is almost as thick as in the absence of NaTC.

Nonlinear Curve Fitting. Typical nonlinear curve fitting plots for AOT reversed micelles containing 5 μM chymotrypsin with no NaTC and with 10 mM NaTC are shown in Figures 2 and 3, respectively. The error bars

Table 2. Results in Heptane from Nonlinear Curve Fitting of log *I* versus log *Q* Plots Using a Polydisperse Spheres Model[a]

sample	R_1	R_2	polydispersity	
			H_2O	D_2O
0 mM NaTC	26.5 ± 0.1	22.5 ± 0.04	0.15 ± 0.003	0.22 ± 0.002
5 mM NaTC	22.1 ± 0.1	19.2 ± 0.03	0.16 ± 0.002	0.39 ± 0.002
10 mM NaTC	29.7 ± 0.1	22.4 ± 0.03	0.18 ± 0.002	
20 mM NaTC	31.6 ± 0.1	22.6 ± 0.009	0.22 ± 0.002	
0 mM NaTC/chymotrypsin	19.2 ± 0.03		0.12 ± 0.002	
10 mM NaTC/chymotrypsin	19.0 ± 0.04		0.25 ± 0.001	

[a] R_1 and R_2 are radii (in Å) of the overall reversed micelles and interior water pools, respectively. The polydispersity (in Å) is given for H_2O cores and D_2O cores. R_2 values for samples with chymotrypsin could not be determined because the core cannot be deuterated. Polydispersity values for D_2O cores at 10 and 20 mM NaTC could not be satisfactorily determined.

represent the standard deviation in the intensity measurement at a particular *Q* value. The solid line represents the curve obtained from the polydisperse spheres model, which provided the best fits to the data.

The large error bars in the high-*Q* region are a result of high instrumental noise. Less weight is given to these points in the fit because of their greater uncertainty. The discrepancy between the model and the scattering data at low *Q* occurs after subtraction of the scattering intensity from the deuterated solvent. As in the high-*Q* region, the uncertainty at low *Q* does not greatly affect the results obtained from the fit, since this region is not significant for the model.

Values for the overall radii, water pool radii, and polydispersity from the nonlinear fits are shown in Table 2. As was observed in the results from Guinier analysis, the sizes of both the overall reversed micelles and the water pools decrease substantially upon addition of 5 mM NaTC and the overall size is greatest at 20 mM NaTC. However, in contrast to the results obtained using Guinier analysis, the size of the water pool is constant with the exception of the decrease at 5 mM NaTC and a smaller thickness is extracted for the surfactant layer in the absence of NaTC.

The distinct oscillations at high *Q* in the plots of log *I* versus log *Q* for the reversed micelles in the absence of NaTC indicate that these aggregates are relatively monodisperse. The oscillations fade as NaTC is added to the system, indicating increasing polydispersity in the overall size of the aggregates with increasing NaTC. This is indicated in Table 2 as well. The deuterated core is significantly polydisperse even in the absence of NaTC and becomes increasingly polydisperse as NaTC is added to the system. This may help to explain why the radii recovered from Guinier analysis tend to be larger than those recovered from nonlinear analysis, since the Guinier method gives more weight to particles with larger dimensions.

The radii obtained from the nonlinear method for reversed micelles with chymotrypsin are considerably smaller than those for unoccupied reversed micelles. A similar trend was observed in the Guinier results although the decrease in size was less pronounced.

Discussion

We have previously observed that low concentrations of NaTC (≤5 mM) appear to disrupt the organization of the AOT detergent layer, while, at higher concentrations, the disruption is diminished and the water capacity of the reversed micelles is increased.[10] Additionally, penetration of bulk organic solvent into the detergent layer was shown to increase with increasing NaTC up to 10 mM and then decrease at higher NaTC. Figure 4 represents two possible orientations of NaTC molecules in the AOT detergent layer.[10] At low concentrations, NaTC monomers may be

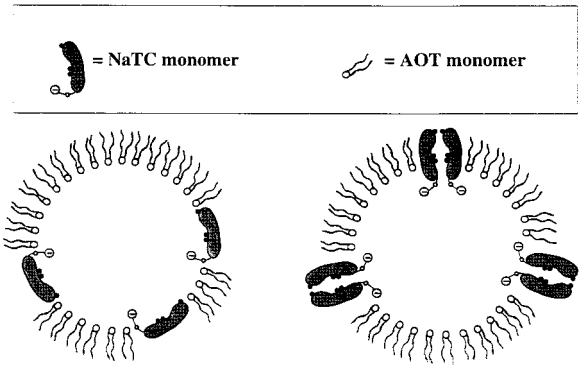

Figure 4. Schematic representation of AOT reversed micelles in the presence of NaTC proposing different orientations of NaTC relative to AOT.

randomly dispersed among the AOT molecules in the detergent layer, oriented perpendicular to the AOT monomers, and lying sidewise across the interface with the hydroxyl-containing surface and hydrophilic tail in contact with the aqueous pool at the micellar core. This would serve to disrupt the organization of the detergent layer and increase solvent penetration, thereby reducing the apparent thickness of the detergent layer extracted from SANS to unrealistically low values. At higher NaTC, hydrogen-bonded NaTC dimers are likely to form. These dimers will be distributed in the detergent layer parallel to the AOT monomers with their hydrophobic surfaces in contact with the AOT tails and their hydrophilic tails oriented toward the aqueous core. This is a more organized structure that could stabilize the detergent layer through hydrophobic interactions and reduce solvent penetration, thereby increasing the apparent detergent layer thickness.

Interestingly, the size of the aggregates decreases in the presence of chymotrypsin. Chymotrypsin is an ellipsoidal protein with exterior dimensions of (40 × 40 × 51) Å^3.[27] Typical radii associated with AOT reversed micelles are on the order of 30 Å, as characterized by quasi-elastic light scattering.[27] Chymotrypsin is likely displacing some of the water in the interior core upon encapsulation, creating a bimodal distribution of sizes between occupied and unoccupied aggregates. A similar phenomenon has been reported for cytochrome *c*.[18] At the enzyme concentration used for this study (5 μM), roughly half of the reversed micelles contain an enzyme molecule. Since the Guinier analysis provides an average particle radius, a bimodal distribution is impossible to characterize by this data analysis method.

In a previous study,[12] we found that increasing ω in the absence of NaTC decreases the catalytic efficiency of

(26) Blow, D. M. *Enzymes* **1971**, *3*, 185.
(27) Nicholson, J. D.; Clarke, J. H. R. *Surfactants in Solution*; Mittal, Lindman, Eds.; Plenum: New York, 1984; Vol. 3.

chymotrypsin. We attributed the decreased activity to the increased size of the water pool, which would behave increasingly like bulk water and decrease the positive effects of reversed micellar encapsulation on the enzymatic activity. Increasing NaTC at constant ω, on the other hand, increased the catalytic efficiency of the enzyme. Since the SANS results indicate a substantial increase in water pool size with added NaTC, yet the effect of NaTC is opposite to that of increasing ω, we can conclude that the mechanism by which NaTC increases catalytic efficiency of chymotrypsin is unrelated to the size of the water pool. Instead, the effect of NaTC is likely due to its effect on the organization and chemical properties of the detergent layer.

Acknowledgment. Financial support for this research was provided by the U. S. Army Research Office, Chemical Sciences Division (Grant DAAH04-93-D-002). The authors also wish to thank the NIST Center for Neutron Research for the use of their facilities.

LA0101797